Available Online at http://www.journalajst.com

ASIAN JOURNAL OF SCIENCE AND TECHNOLOGY

ISSN: 0976-3376

Asian Journal of Science and Technology
Vol. 07, Issue, 11, pp.3842-3849, November, 2016

RESEARCH ARTICLE

A NOVEL MAGNETIC ACTIVATED CARBON PRODUCED VIA HYDROCHLORIC ACID PICKLING WATER ACTIVATION FOR METHYLENE BLUE REMOVAL

***Fang Wang**

Key Laboratory of Materials Chemistry in Binzhou City, Department of Chemical Engineering, Binzhou, University, Binzhou, 256600, Shandong Province, China

ARTICLE INFO

Article History:
Received 27th August, 2016
Received in revised form
14th September, 2016
Accepted 19th October, 2016
Published online 30th November, 2016

Key words:

Peanut shell,
Magnetic activated carbon,
Hydrochloric acid pickling water,
Methylene.

ABSTRACT

A novel biomass-based and low cost magnetic activated carbon (MAC) was synthesized from a peanut shell via a simple one-step method using hydrochloric acid pickling water as an activating agent. The effectiveness of MAC in the removal of methylene blue (MB) has been investigated extensively. The morphology and surface chemistry of the obtained MAC were characterized by Fourier transform infrared (FT-IR), X-ray diffraction spectra (XRD), scanning electron microscopy (SEM) and Brunauer–Emmett–Teller (BET) surface area. A batch adsorption study was performed at varying pH levels, dye concentrations, temperatures, and adsorbent doses. In order to examine the adsorption kinetic and the mechanism of adsorption, pseudo-first-order, pseudo-second-order and intra-particle diffusion models were fitted. It was found that the equilibrium data were best represented by the Langmuir isotherm, with the maximum monolayer adsorption capacity of 201.61 mg/g at 298 K. The adsorption kinetic followed a pseudo-second-order equation. Thermodynamic study showed that the adsorption was a spontaneous and endothermic process.

INTRODUCTION

Biomass activated carbon can be regard as one of the most commonly adsorbents because of its abstractive advantages, such as low cost, high specific surface area, and high porosity. It has been widely prepared by different activators such as H_3PO_4 (Royer *et al*., 2009), $ZnCl_2$ (Rufford *et al*., 2010; Avealr *et al*., 2010), KOH (Balathanigaimani *et al*., 2008; Tan *et al*., 2008), H_2SO_4 (Malarvizhi and Ho, 2010) or $FeCl_3$ (Samar and Muthanna, 2012; Rufford *et al*., 2010). However, the conventional biomass activated carbon often suffers from separation in liquid–solid phase processes except high speed centrifugation or filter. Fortunately, the magnetic-assisted separation technology can provide an alternative approach to overcome the difficulty in separation and recovery of conventional powdery adsorbents from an adsorption solution (Hristov and Fachikov, 2007). By far, the conventional two step method is mainly used to prepare magnetic activated carbon (MAC) (Zhu *et al*., 2010; Tan *et al*., 2007; Ma *et al*., 2015). However, the two-step method has several disadvantages, such as complexity, high cost process and the loss of adsorption capacity during recycle (Zhang *et al*., 2015).

Corresponding author: Fang Wang,
Key Laboratory of Materials Chemistry in Binzhou City, Department of Chemical Engineering, Binzhou, University, Binzhou, 256600, Shandong Province, China.

In steel industries, the pickling process generates a considerable amount of hydrochloric acid pickling water containing the dissolved metal salts of iron, chromium and nickel as well as residual free acids. According to United State Environmental Protection Agency (USEPA), the waste generated by the metal pickling and the electroplating industries is identified as hazardous solid waste (Devi *et al*., 2014). If one could combine the advantages of cheap agricultural residues and magnetic activators, such as $FeCl_3$ and HCl in hydrochloric acid pickling water, fabricate a nanocomposite with high surface area, appropriate pore size, and magnetic separability, a promising novel adsorbent may be accessible. To our best knowledge, MAC prepared from peanut shells using hydrochloric acid pickling water as an activating agent has not yet been explored. The aim of this study is to develop the method for preparation of MAC with higher adsorption capacity and excellent separation properties from peanut shells using hydrochloric acid pickling water as activator. Methylene Blue (MB) was selected as the model pollutant to study adsorption kinetics and the thermodynamics of the pollutant onto MAC under different experimental conditions. The method to be developed in this paper will help to minimize the environmental pollution in dye wastewater treatment and also maximize the economic value of the agricultural wastes and the industrial wastes (stainless steel pickling water).

MATERIALS AND METHODS

Preparation of MAC

The peanut shell locally was first washed with distilled water, dried, cut and sieved to 1-2 mm. Twenty grams of peanut shell was impregnated with 500 mL hydrochloric acid pickling water (the composition was shown in Table 1) for 24 h, and then dry in a muffle furnace at 393 K for 12 h to prepare the impregnated sample. Subsequently, the impregnated sample was heated up at a ramping rate of 10 K/min in a nitrogen flow and carbonized at different activation temperatures (773, 973 and 1023 K). After, the activated carbon was cooled to room temperature with continuous nitrogen flush. The cooled solid was washed by the deionized water and filtered several times until the pH value of the filtrate reached neutral. Finally, the samples were dried for testing and were represented as MAC (773), MAC (973) and MAC (1023).

The yield of activated carbon was calculated using the following equation:

$$Y\% = \frac{W_0}{W_f} \times 100\% \quad (1)$$

where W_f and W_0 are the weight of final activated carbon product(g) and the weight of the dried peanut shell (g), respectively.

Characterization of adsorbent

The functional carbon-oxygen groups on the surface of the MAC were identified by using FT-IR technique and XRD. The MAC was diluted with KBr, and the FT-IR spectra were acquired by an AVATAR 360 (Thermo Nicolet Co., USA) FTIR spectrophotometer. The X-ray diffraction spectra (XRD) were measured using a Bruker D8 advanced X-ray diffractometer with Cu Kα radiation (λ= 1.5406 Å) in the scanning angle range of 10–90^o at a scanning rate of 10 ^{o} /min at 40mA and 40 kV. The specific surface area and mesoporous structure of the adsorbents were measured by the Brunauer-Emmett-Teller (BET) method on a Micromeritics ASAP-2020 apparatus at liquid nitrogen temperature with N_2 as the absorbent at 77 K. Scanning electron microscopy (SEM) analysis was carried out by JSM-6490LV for the obtained activated carbon to study their surface textures and the development of porosity.

Adsorption studies

Batch equilibrium experiments were carried out in a set of Erlenmeyer flasks (250 mL) where 100 mL of MB solutions with varying initial concentrations of 90–450 mg/L. The original pH of the solutions was around 6.5. In order to minimize the interference of the carbon fines with the analysis, all samples were filtered prior to analysis. The concentrations of MB after adsorption were determined using a T6 UV–vis spectrophotometer (Beijing, China) at 664 nm. The amount of adsorption at equilibrium, q_e (mg/g) was defined by the following formula,

$$q_e = \frac{(C_0 - C_e)V}{W} \quad (2)$$

where C_0 and C_e (mg/l) are the liquid-phase concentrations of MB at the initial time and equilibrium, respectively. V is the volume of the solution (l) and W is the mass of dry MAC used (g).

RESULTS AND DISCUSSION

Characterization of materials

N_2 adsorption-desorption isotherms (Fig.1) and detailed data of the yield, BET surface area and average pore diameter value of the obtained MAC prepared at different temperatures are summarized in Table 2. It can be found that increasing activation temperature progressively from 773 to 1023 K reduces the yield of the activated carbon from 63.75% to 45.72%. In addition, we find that BET surface areas decrease with the increasing activated temperature and time. The N_2 adsorption-desorption isotherms of MAC belong to type III profile, reveal the pore size distribution in the range of mesoporous, which are advantageous for mass transfer between dye molecular and the adsorbent. To characterize surface groups on activated carbon, FT-IR spectra of the attained activated carbon are measured and shown in Fig. 2. The infrared spectra for MAC suggest the complete carbonization of the material, which can be characterized by the complete disappearance of the bands associated with C-H stretching, at 2928 and 2855 cm^{-1} (Oliveiraa *et al*., 2009). The wide band at around 3442cm^{-1} is a consequence of O-H groups and adsorbed water. The peak at 1599 cm^{-1} and 1642 cm^{-1} are the signature of the C=O stretching vibration of lactonic and carbonyl groups. The peak occurring at 1121 cm^{-1} is ascribed to oxygen functional groups such as highly conjugated C-O stretching, C-O stretching in carboxylic groups, and carboxylate moieties. In addition, there are two obvious absorbent bands at the low frequency zone of 502 cm^{-1} and 594 cm^{-1}, which are assigned to the stretching vibration of the Fe-O bond in magnetite (Franger *et al*., 2006). In order to evaluate the structure of the carbon phase and iron oxides, X-ray diffraction patterns of the MAC prepared at different activation temperature are shown in Fig.3. The X-ray diffraction patterns of the MAC display a number of sharp peaks which are compatible with the presence of α-FeO(OH) (peaks at 21.0 and 33.5 degrees), Fe_2O_3 (hematite) (peaks at 32.5, 37.5, 38.8 and 42.3 degree) and Fe_3O_4 (magnetite) (peaks at 30.1, 35.4, 43.1, 56.9, and 62.5 degree) (Oliveira *et al*., 2002). According previous reports, hematite and magnetite are magnetic with magnetizations of 100 and 60 J·T·kg (Oliveira *et al*., 2000). Therefore the obtained MAC is magnetic and can be separated easily from waste water. To observe the morphology of the prepared samples, the scanning electron microscopy-SEM is shown in Fig. 4. Many large pores in a honeycomb shape are clearly found on the surface of the activated carbon. The well-developed pores have led to the large surface area and porous structure of the activated carbon, which are in accordance with BET results. These results show that $FeCl_3$ and HCl in hydrochloric acid pickling water are effective in creating well-developed pores on the surface of the precursor, hence leading to the activated carbon with large surface area and porous structure.

Adsorption experimental studies

Effect of MAC(973) dosage on MB adsorption

The effect of MAC dosage on MB adsorption capacity is shown in Fig. 5. It can be found that the removal percentage

increases rapidly with an increase of MAC dosage, and the removal percentage almost reaches a constant value of 92.5 % after the critical dosage of 0.06 g. However, the adsorption amount of MB drops as the dosage of MAC increases. This may be attributed to the increase in the availability of surface active sites resulting from the increased dosage and conglomeration of the adsorbent. When we further increased the dosage of MAC to 0.10 g, the removal percentage of MB showed no significant difference.

Effect of solution initial pH on MB uptake

The pH of the aqueous solution is an important factor influencing the dye adsorption process by way of changing the surface charge of an adsorbent and the ionization behavior of the adsorbent and the dye (Qada *et al*., 2006). The relation influences between solution pH on the adsorption amounts and removal percentages of MB are shown in Fig. 6. It is noticeable that Qe is relatively low at acidic conditions, and the maximum is obtained at about pH = 7. The adsorption of MB onto the obtained MAC(973) is not drastically influenced when the solution pH increased from 7 to 11. The result indicates that the surface of MAC(973) is negatively charged. The negatively charged surfaces can enhance the adsorption capacity of the positively charged MB cations by the adsorbents through electrostatic forces of attraction (Hameed and Ahmad, 2009).

Effect of contact time and initial concentration

Equilibrium time is one of the most important parameters in the design of initial economical wastewater treatment references. To investigate the kinetics of adsorption, three different concentrations of MB were chosen, those being 270 mg/L, 360 mg/L and 450 mg/L. As can be seen in Fig.7, the adsorption is initially rapid and then slows down. The time required for equilibrium adsorption of MB is about 5 h. It is possible that a large number of vacant surface sites are available for adsorption during the initial stage and the remaining vacant surface sites are difficult to occupy due to the repulsive forces between the MB molecules on the MAC and the bulk phase (Hsin, 2007). In addition, the adsorption amount of MB increases from 176.45 mg/g to 197.25 mg/g when the initial concentration is increased from 270 mg/L to 450 mg/L. This result indicates that it is very important for the initial concentration in the adsorption capacity of MB on the obtained MAC. This may be attributed to an increase in the driving force of concentration gradient with an increase in the initial concentration. Finally, the curves are single, smooth and continuous towards saturation, indicating the formation of monolayer coverage of MB molecules on the MAC surface (Malik, 2003).

Effect of temperature on adsorption capacity of activated carbon

Temperature is an important parameter for the adsorption process and batch adsorption studies were carried out at three different temperatures, namely 298, 308 and 318 K, over a range of initial MB concentrations. The effect of the temperature on the adsorption in terms of adsorption isotherms are shown in Fig.8. It can be found that the adsorption amount of MB on MAC(973) increases with increasing equilibrium MB concentrations in the range of experimental concentration. The results due to the active sites of MAC are surrounded by a larger number of MB ions when the concentration of MB in solution was greater. In addition, it is observed that the adsorption amounts increase with increase in temperature, indicating the endothermic nature of the adsorption reaction of MB onto MAC.

Adsorption isotherms

Adsorption equilibrium isotherm model equations such as Langmuir and Freundlich were used in this study to describe the experimental adsorption data. The linear form of Langmuir isotherm and Freundlich equation are given as:

$$\frac{C_e}{q_e} = \frac{1}{Q_0 b} + \frac{1}{Q_0} C_E \quad (3)$$

$$\log q_e = \log K_F + \frac{1}{n} \log C_e \quad (4)$$

where C_e is the equilibrium concentration of the adsorbate (mg/L), q_e is the amount of adsorbate adsorbed per unit mass of adsorbent (mg/g), Q_0 and b are Langmuir constants related to adsorption capacity and rate of adsorption, respectively. K_F and n are Freundlich constants with n giving an indication of how favorable the adsorption process. K_F (mg/g (l/mg)) is the adsorption capacity of the adsorbent, which can be defined as the adsorption or distribution coefficient, and represents the quantity of dye adsorbed onto activated carbon for a unit equilibrium concentration.

For the Langmuir isotherm at 298, 308 and 318 K, when C_e/q_e is plotted against C_e, three straight lines with slope of $1/Q_0$ are obtained, as shown in Fig.9. All the constants and the linear correlation coefficient R^2 of the two isotherm models used are summarized in Table 3. The Langmuir model yields a better fit with R^2 values higher than 0.99, as compared to the Freundlich isotherm model. The result shows that during the adsorption process the uptake of MB occurs on a homogenous surface by monolayer adsorption without any interaction between adsorbed MB.

The value of separation factor R_L can be obtained from the following equation (Weber and Chakkravorti, 1974):

$$R_L = \frac{1}{1 + K_L C_0} \quad (5)$$

where C_0 is the highest initial dye concentration, mg L^{-1}. It should be noted that the values of R_L at temperature of 298 K, 308 K and 318 K are 0.036, 0.031 and 0.028, respectively. The values of R_L indicate the favorability of MB adsorption on the obtained MAC under the conditions used in this study (Arivoli *et al*., 2008). As can be seen from Fig.10, for the Freundlich isotherm, the slopes of 1/n at 298 K, 308 K and 318 K are 0.26, 0.26 and 0.28, respectively. This result indicates that MB adsorption on MAC prepared in this work is a normal Langmuir isotherm (Fytianos *et al*., 2000).

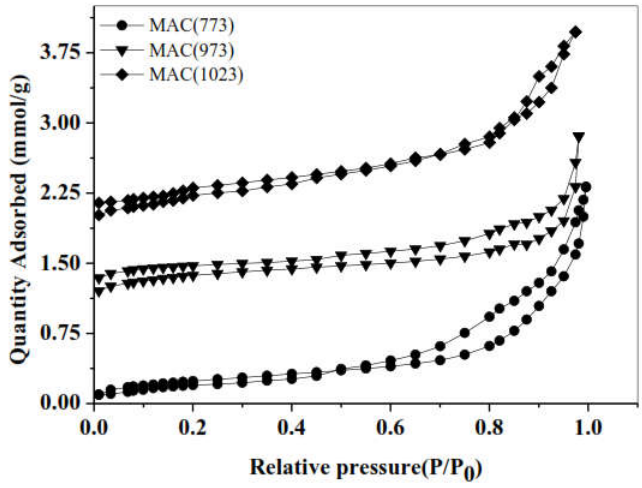

Fig.1. N_2 adsorption-desorption isotherms

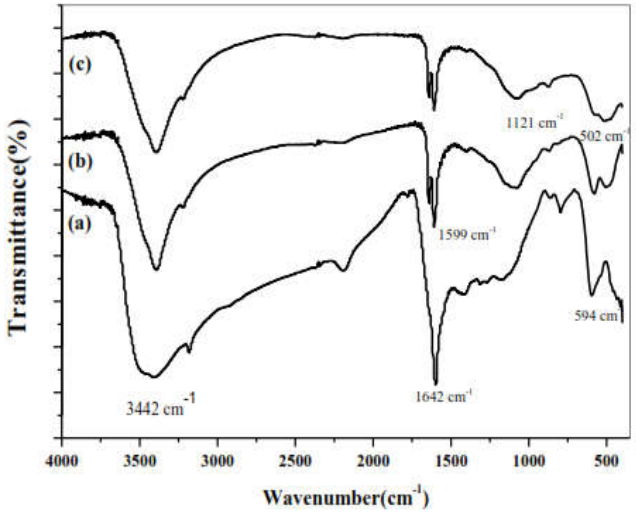

Fig.2. FT-IR spectra of activated carbon before adsorption. (a) MAC (773), (b) MAC (973) and (c) MAC (1023)

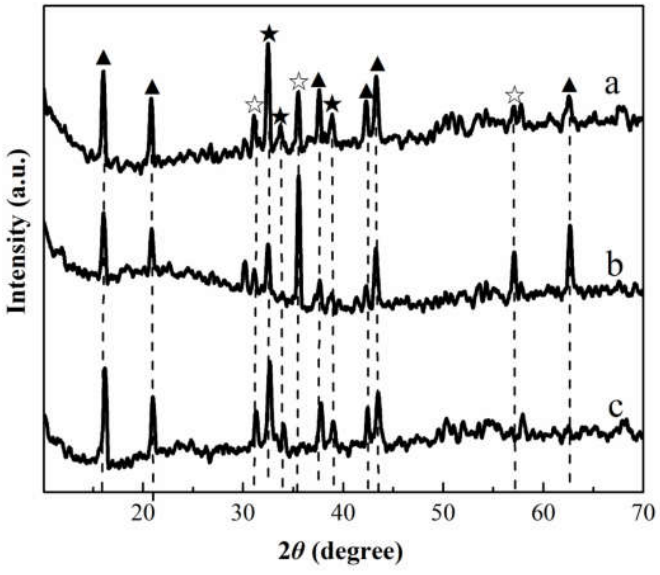

Fig.3. X-ray powder diffraction patterns for (a) MAC (773), (b) MAC (973) and (c) MAC (1023) (▲a-FeO(OH), ☆:Fe_3O_4, ★:Fe_2O_3)

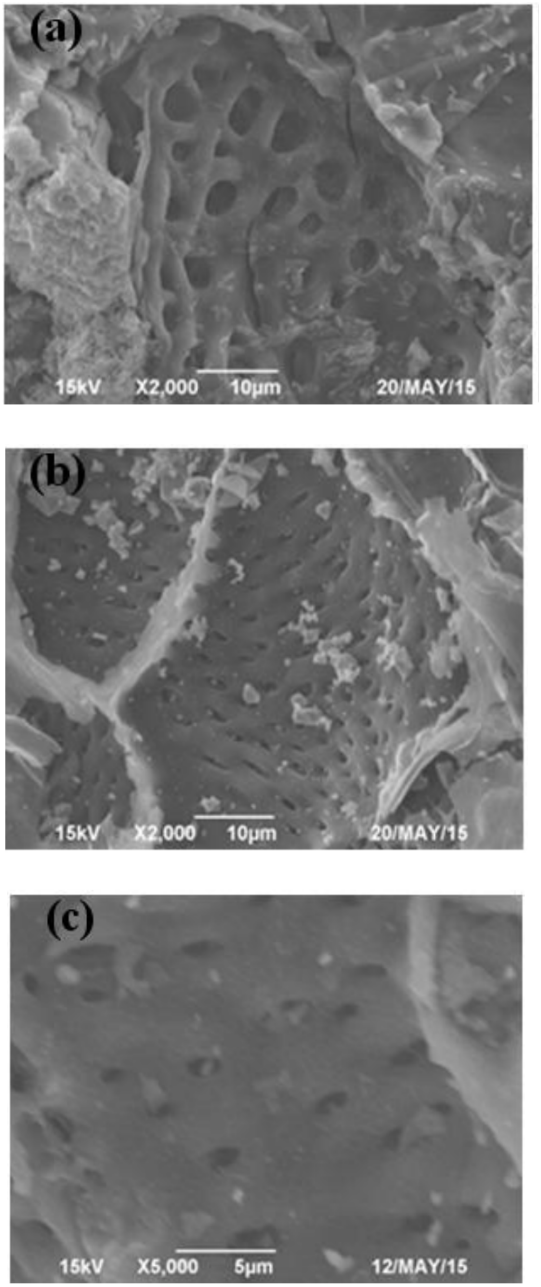

Fig.4. SEM images for activated carbon carbonized at different temperatures (a) MAC (773), (b) MAC (973) and (c) MAC (1023)

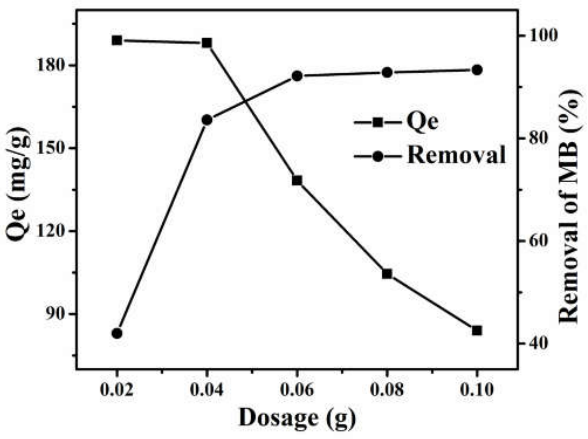

Fig.5. Effect of adsorbent dosage on the removal of MB onto MAC (MB concentration 450 mg/L, temperature 25±2 °C, contact time 360 min)

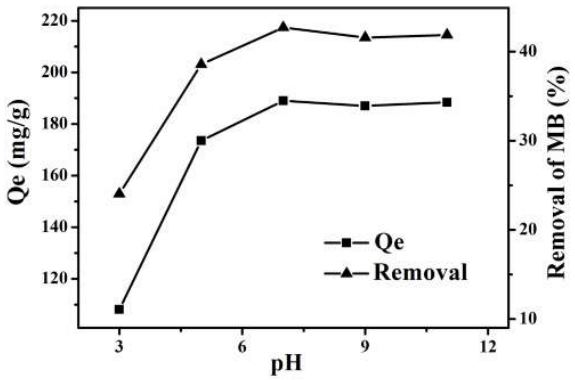

Fig.6. Effect of pH on the adsorption of MB (initial concentration is 450 mg/g - equilibrium time is 6 h, temperature is 298 K)

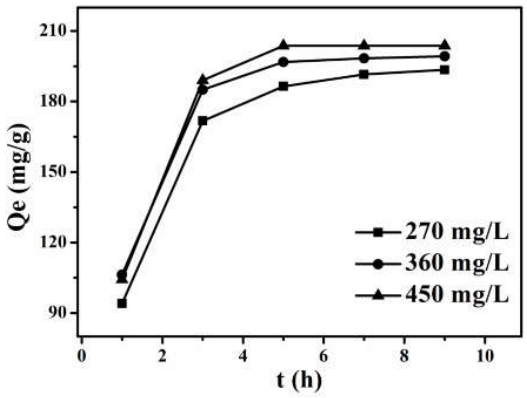

Fig.7. Effect of contact time and initial MB concentration (natural pH, temperature 25±2 °C)

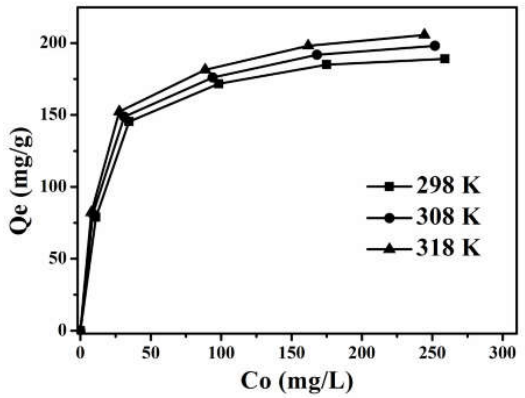

Fig.8. Effect of temperature on adsorption of MB onto MAC (natural pH)

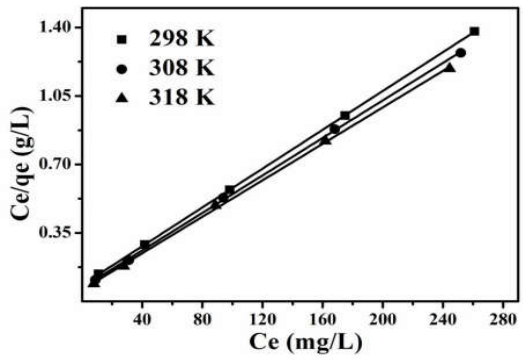

Fig.9. Langmuir adsorption isotherm of MB onto MAC at 298 K, 308 K and 318 K

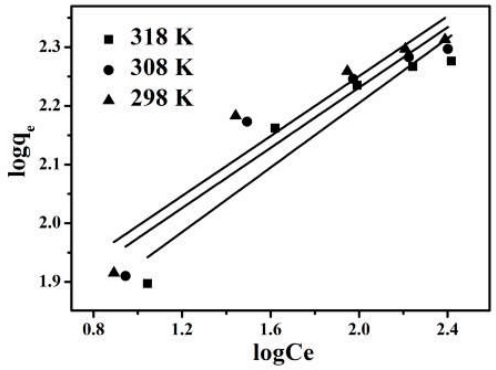

Fig.10. Freundlich adsorption isotherm of MB onto activated carbon at 298 K, 308 K and 318 K

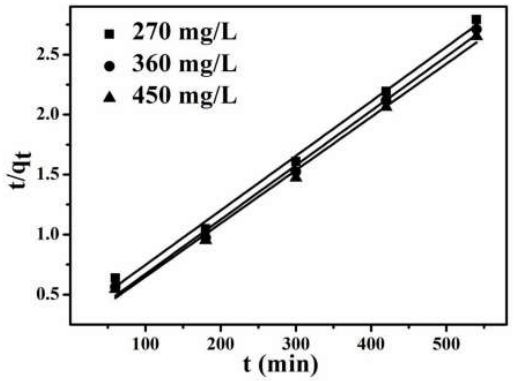

Fig.11. Pseudo-second-order kinetics for adsorption of methylene blue onto MAC at 298 K

In addition, the maximum monolayer adsorption capacity of MB at 298K, 303 K and 313 K are 201.61 mg/g, 208.77 mg/g, and 214.59 mg/g. The MAC obtained in this work has a relatively large adsorption capacity when compared to some data obtained from the literature for activated carbons prepared from various activators (Zhou *et al*., 2015; Hall *et al*., 1966). The high adsorption capacity of the activated carbon prepared in this study could be due to its relatively high surface area and its mesoporous structure. It can be determined that the hydrochloric acid pickling water can be classified as one of the effective activators for this purpose.

Adsorption kinetics

In order to investigate the kinetics of adsorption of MB on the adsorbents, various kinetic models, like pseudo-first-order, pseudo-second-order and intraparticle diffusion models were used.

These models can be expressed as:

$$\ln(q_e - q_t) = \ln q_e - k_1 t \quad (6)$$

$$\frac{t}{q_t} = \frac{1}{k_2 q_e^2} + \frac{1}{q_e} t \quad (7)$$

$$q_t = k_p t^{1/2} + C \quad (8)$$

where q_e and q_t (mg/g) are, respectively, the uptake of MB at equilibrium and at time t (min), K_1 (1/min) is the adsorption rate constant, K_2 (g/mg min) is the rate constant of second-order equation,

Table 1. Composition of hydrochloric acid pickling water

Component composition	(g/L)
Free HCl	160-180
Fe(III)	140-145
Ni(II)	3-5

Table 2. Yield, surface area, and pore size of MAC at different activation temperatures

Activation conditions	Yield (%)	BET surface area(m^2/g)	Pore size (nm)
773-1	63.75	758	38
973-1	52.32	932	23
1023-1	45.72	843	18
1023-1.5	42.58	802	14

Table 3. Langmuir and Freundlich isotherm model constants for adsorption of MB onto MAC

Temperature(K)	Langmuir isotherm				Freundlich isotherm		
	Q_L (mg/g)	K_L (L/mg)	R_L	R^2	K_F(mg/g)(L/mg)	1/n	R^2
298	201.61	0.0596	0.036	0.9999	55.20	0.26	0.8721
308	208.77	0.0696	0.031	0.9996	52.21	0.26	0.8745
318	214.59	0.0784	0.028	0.9992	45.14	0.28	0.8827

Table 4. Comparison of the pseudo- rst-order kinetic, pseudo-second-order kinetic and intraparticle diffusion models for different initial MB concentration at 298 K

Co	$q_{e,exp}$	Pseudo-first-order kinetic			Pseudo-second-order kinetic			Intraparticle diffusion	
(mg/L)	(mg/g)	$q_{e,cal}$(mg/g)	K_1(min^{-1})	R^2	$q_{e,cal}$(mg/g)	K_2(min^{-1})	R^2	K_3(g/(mg•min))	R^2
270	193.47	76.327	-0.2408	0.9693	220.264	$9.5x10^{-5}$	0.9932	47.9138	0.6628
360	199.20	78.256	-0.3344	0.9648	220.750	$9.4x10^{-5}$	0.9937	44.1947	0.6711
450	204.03	90.736	-0.5760	0.7721	225.734	$7.0x10^{-5}$	0.9940	47.7161	0.7430

Table 5. Thermodynamic parameters for adsorption of MB onto prepared MAC

Co	ΔH◦ (J/mol)	ΔS◦ (J/mol K)	ΔG◦ (J/mol)		
(mg/L)			298	308	318
90	53171.81	161.85	-4866.72	-5689.83	-6228.50
180	10236.03	46.32	-3556.12	-4000.72	-4510.27
270	6046.52	24.92	-1380.82	-1605.59	-1895.28

K_3 (mg/g $min^{1/2}$) is the intraparticle diffusion rate constant, and C (mg/g) is a constant that corresponds to the thickness of the boundary layer. Comparison of the pseudo-first-order kinetic, pseudo-second-order kinetic and intraparticle diffusion models for different initial MB concentration at 298 K are summarized in Table 4. As shown in Fig.11, the linear plot of t/q_t versus t shows a good agreement between the experimental and the calculated q_e values. Additionally, based on the highest R^2 values that were greater than 0.999 for all MB concentrations, the pseudo-second-order model is the most suitable equation to describe the adsorption kinetics of MB on the prepared MAC. This suggests that the overall rate of the adsorption process is controlled by chemisorption which involves covalent forces through sharing or exchange of electrons between the MAC and MB (Ma *et al*., 2015). From Table 4, the values of rate constant K_2 decrease with increasing initial concentration of MB. The reason for this behavior can be attributed to the high competition for the adsorption surface sites at high concentration which leads to higher sorption rates.

Adsorption thermodynamics

The thermodynamic parameters that determine the process are changes in standard enthalpy (ΔH^o), standard entropy (ΔS^o) and standard free energy (ΔG^o) due to the transfer of one unit mole of solute from solution onto the solid–liquid interface. The value of ΔH^o and ΔS^o are computed using the following equation:

$$Kd = \frac{qe}{Ce} \quad (9)$$

$$\frac{\Delta S^o}{} \quad \frac{\Delta H^o}{} \quad (10)$$

$$\ln Kd = {}_{R} \; {}^{-} RT$$

$$\Delta G^{O} = -RT \ln K \quad (11)$$

d

where K_d is the distribution coefficient, q_e (mg/L) is the amount adsorbed on solid at equilibrium and Ce (mg/L) is the equilibrium concentration. R (8.314 J/mol K) is the universal gas constant, and T (K) is the absolute solution temperature; The calculated values of ΔH , ΔS and ΔG at 298 K, 308 K and 318 k are summarized in Table 5. The negative value of ΔG indicates the feasibility of the process and the spontaneous nature of the adsorption with a high preference of MB onto the prepared MAC. The positive value of ΔH indicates the endothermic nature of the adsorption interaction. As can be seen from Table 2, the maximum monolayer adsorption amounts of MB increased from 201.61 to 214.59 mg/g with increasing temperature. This result confirms the adsorption process of MB on MAC is endothermic. Finally, the positive value of ΔS shows the affinity of the obtained MAC for MB and the increasing randomness at the solid-solution interface during the adsorption process.

Conclusion

MAC was synthesized successfully from a peanut shell using hydrochloric acid pickling water as an activating agent. The MAC obtained at 973 K shows a relatively high surface area (932 m^2/g) and a porous honeycomb structure, which is identified to be an effective adsorbent for the removal of MB from aqueous solutions. Adsorption parameters for the Langmuir and Freundlich were determined and the equilibrium data were best described by the Langmuir isotherm model. The adsorption kinetics can be successfully fitted to pseudo-second-order kinetic model. Thermodynamic study showed that the adsorption was a spontaneous and endothermic process. For a better understanding of the properties of these activated carbons, it is necessary to expand this work to include optimization of the parameters in activated carbon preparation progress and the adsorption of other potentially polluting molecules.

Acknowledgments

The Shandong Natural Science Foundation of China (ZR2014BL014), a Project of Shandong Province Higher Educational Science and Technology Program (J14LC54), a Project of Binzhou City science and technology development project (2014ZC0212) and Binzhou University (BZXYFB20140806 and 2010Y06.) research Funds are acknowledged for support of the research.

REFERENCES

Arivoli, S., M. Hema, M. Karuppaiah, S. Saravanan, 2008. Adsorption of chromium ion by acid activated low cost carbon-kinetic, mechanistic, thermodynamic and equilibrium studies, *E.J. Chem*., 5;820-831.

Avealr, F.F., M.L. Bianchi, M. Goncalves, E.G. de Mota, 2010. The use of piassava fibers (Attalea funifever) in the preparation of activated carbon, *Bioresour. Technol*., 101; 4639-4645.

Balathanigaimani, M.S., S. Wag-Guen, M.J. Lee, C.H. Kim, J.W. Lee, H. Moon, 2008. Highly porous electrodes from novel corn grains-based activated carbons for electrical double layer capacitors, *Electrochem. Commun*., 10; 868-871.

Ch Zhou, L., J.J Ma, H. Zhang, Y.M Shao, Y.F Li. 2015. Fabrication of magnetic carbon composites from peanut shells and its application as a heterogeneous Fenton catalyst in removal of methylene blue, *Appl. Sur. Sci*., 324; 490-498.

Ch. Hsin, W. 2007. Adsorption of reactive dye onto carbon nanotubes: equilibrium, kinetics and thermodynamics, *J. Hazard. Mater*. 144;93-100.

Devi, A., A. Singhal, R. Gupta, P. Panzade, 2014. A study on treatment methods of spent pickling liquor generated by pickling process of steel, Clean. Techn. Environ. Policy. 16; 1515-1527.

Franger, S., P. Berthet, O. Dragos, R. Baddour-Hadjean, P. Bonville, J. Berthon, 2006. Large influence of the synthesis conditions on the physio-chemical properties of naostructured Fe_3O_4, *J. Nanopart. Res*., 9;389-402.

Fytianos, K., E. Voudrias, E. Kokkalis, 2000. Sorption-desorption behavior of 2,4-dichlorophenol by marine sediments, *Chemosphere*, 40;3-6.

Hall, K.R., L.C. Eagleton, A. Acrivos, T. Vermeulen, 1966. Pore- and solid-diffusion kinetics in fixed-bed adsorption under constant-pattern conditions, *Ind. Eng. Chem. Fundam*., 5;212-223.

Hameed, B.H., A.A. Ahmad, 2009. Batch adsorption of methylene blue from aqueous solution by garlic peel, an agricultural waste biomass, *J. Hazard. Mater*., 164;870–875.

Hristov, J. and L. Fachikov, 2007. An overview of separation by magnetically stabilized beds: state-of-the-art and potential applications, *China Particuology*., 5; 11-18.

Ma, J.J., L.Ch. Zhou, W.F. Dan, H. Zhang, Y.M. Shao, C.Bao, L.G. Jing. 2015. Novel magnetic porous carbon spheres derived from chelating resin as a heterogeneous Fenton catalyst for the removal of methylene blue from aqueous solution. *J. Colloid Interface Sci*., 446;298-306.

Malarvizhi, R., Y.S. Ho, 2010. The influence of pH and the structure of the dye molecules on adsorption isotherms modeling using activate carbon, *Desalination*. 264;97-101.

Malik, P.K. 2003. Use of activated carbons prepared from sawdust and rice-husk for adsorption of acid dyes: a case study of Acid Yellow 36, Dyes Pigments. 56;239-249.

Oliveira, L.C., R.V. Rios, J.D. Fabris, V. Garg, K.Sapag, R.M.Lago, 2002. Activated carbon/iron oxide magnetic composites for the adsorption of contaminants in water. Carbon, 40, 2177 2183.

Oliveira, L.C.A., J.D. Fabris, W.N. Mussel *et al*. 2000. The effect of Mn substitution on the catalytic properties of ferrites. *Stud Surf Sci Catal*., 130;2165-2168.

Oliveiraa, L.C.A., E. Pereiraa, I. R. Guimaraesa, A. Vallone, M. Pereirac, J.P. Mesquitac, K. Sapag, 2009. Preparation of activated carbons from coffee husks utilizing $FeCl_3$ and $ZnCl_2$ as activating agents, *J.Hazard. Mater*., 165;87-94.

Qada, E.N.E., S.J. Allen, G.M. Walker, 2006. Adsorption of methylene blue onto activated carbon produced from steam activated bituminous coal: a study of equilibrium adsorption isotherm, *Chem. Eng. J*., 124;103-110.

Royer, B., N.F. Cardoso, E.C. Lima, J.C.P. Vaghetti, R.C. Veses, 2009. Applications of Brazalin pine-fruit shell in natural and carbonized forms as adsorbents to removal of methylene blue from aqueous solutions: kinetics and equilibrium study, *J.Hazard. Mater.*, 164;1213-1222.

Rufford, T.E., D. Hulicova-Jurcakova, K. Khosla, Z. Zhu, G.Q. Lu, 2010. Microstructure and electrochemical double-layer capacitance of carbon electrodes prepared by zinc chloride activation of sugar cane bagasse, *J. Power Sources*, 195;912-918.

Rufford, T.E., D. Hulicova-Jurcakova, Z. Zhu, G.Q. Lu, 2010. A comparative study of chemical treatment by $FeCl_3$, $MgCl_2$, and $ZnCl_2$ on microstructure, surface chemistry, and double-layer capacitance of carbons from waste biomass, *J. Mater Res*., 25;1451-1459.

Samar, K.T., J.A. Muthanna, 2012. Adsorption of methylene blue onto biomass-based activated carbon by $FeCl_3$ activation: Equilibrium, kinetics, and thermodynamic studies, *J. Anal. Appl. Pyrol*., 97;116-122.

Sh. L. Zhang, L.H. Tao, M. Jiang, G. J. Gou, Z.W. Zhou. 2015. Single-step synthesis of magnetic activated carbon from peanut shell. *Mater. Lett*. 157;281-284.

Tan, I.A.W., A.L. Ahmad, B.H. Hameed, 2008. Adsorption of basic dye using activated carbon prepared from oil palm shell: batch and fixed bed studies, *Desalination*, 225;13-28.

Tan, I.A.W., B.H. Hameed, A.L. Ahmad, 2007. Equilibrium and kinetic studies on basic dye adsorption by oil palm fibre activated carbon. Chem. Eng. J, 127;111–119.

Weber, T.W. R.K. Chakkravorti, Pore and solid diffusion models for fixed bed adsorbers, *AIChE J*., 20 (1974) 228-238.

Zhu, H.Y., R. Jiang, L. Xiao, G.M. Zeng, 2010. Preparation, characterization, adsorption kinetics and thermodynamics of novel magnetic chitosan enwrapping nanosized γ-Fe_2O_3 and multi-walled carbon nanotubes with enhanced adsorption properties for methyl orange. *Bioresource Technology*, 101;5063–5069.

****